Osteoinductive ceramics as a synthetic alternative to autologous bone grafting

Huipin Yuan[a,b,1], Hugo Fernandes[b,1], Pamela Habibovic[b], Jan de Boer[b], Ana M. C. Barradas[b], Ad de Ruiter[c], William R. Walsh[d], Clemens A. van Blitterswijk[b], and Joost D. de Bruijn[a,e,2]

[a]Progentix Orthobiology BV, Professor Bronkhorstlaan 10-D, 3723 MB Bilthoven, The Netherlands; [b]MIRA Institute for Biomedical Technology and Technical Medicine, Department of Tissue Regeneration, University of Twente, P.O. Box 217, 7500 AE, Enschede, The Netherlands; [c]Department of Oral and Maxillofacial Surgery, University Medical Center, 3584 CX Utrecht, The Netherlands; [d]Surgical and Orthopaedic Research Laboratories, University of New South Wales, Prince of Wales Hospital, Randwick, New South Wales 2031, Australia; and [e]School of Engineering and Materials Science, Queen Mary University of London, London E1 4NS, United Kingdom

Edited* by Robert Langer, Massachusetts Institute of Technology, Cambridge, MA, and approved June 16, 2010 (received for review March 20, 2010)

Biomaterials can be endowed with biologically instructive properties by changing basic parameters such as elasticity and surface texture. However, translation from in vitro proof of concept to clinical application is largely missing. Porous calcium phosphate ceramics are used to treat small bone defects but in general do not induce stem cell differentiation, which is essential for regenerating large bone defects. Here, we prepared calcium phosphate ceramics with varying physicochemical and structural characteristics. Microporosity correlated to their propensity to stimulate osteogenic differentiation of stem cells in vitro and bone induction in vivo. Implantation in a large bone defect in sheep unequivocally demonstrated that osteoinductive ceramics are equally efficient in bone repair as autologous bone grafts. Our results provide proof of concept for the clinical application of "smart" biomaterials.

osteoinduction | bone morphogenetic proteins | mesenchymal stromal cells | surface topography | tricalcium phosphate

The role of biomaterials as medical devices is changing from a biologically passive, structural role to one in which the properties of the material will orchestrate the process of tissue regeneration. The change is fed by an increasing number of reports demonstrating that cellular behavior can be modulated by material properties such as surface texture, elasticity, and chemistry (1–5). For instance, in the area of biomaterials for the restoration of bone defects, it has been reported that surface topography influences osteogenesis and proliferation of bone marrow-derived multipotent mesenchymal stromal cells (MSCs) in vitro (6, 7). Although tissue instructive materials hold great potential as off-the-shelf bioactive medical devices, so far the concept has not progressed beyond the proof-of-concept phase in which in vitro assays demonstrate an effect on cellular differentiation or proliferation (8). Consequently, transplantation of autologous bone is still the golden standard in bone repair strategies. Autografts guide the in-growth of osteoblasts, the primary cell type responsible for bone matrix apposition, from the adjacent tissues into the defect, a process referred to as osteoconduction. In addition, autologous bone induces de novo bone formation by triggering the differentiation of undifferentiated progenitor cells into the osteogenic lineage, referred to as osteoinduction (9, 10). The latter phenomenon is essential for the repair of large critical-size bone defects. Drawbacks of autografting are the limited availability of autologous bone and the negative side effects of bone harvesting, which make the search for bone graft substitutes an area of intense research (11).

The discovery that osteoinduction can be accomplished by devitalized demineralized bone matrix (DBM) and the subsequent identification of bone morphogenetic proteins (BMPs) provided an alternative to bone autografts (9). Both DBM and BMPs are broadly applied in the clinic, but their biological nature has implications for the production process leading to rather high batch variability and high production costs (12–15). Moreover, the in vivo delivery of soluble molecules such as BMPs is inefficient. An alternative to the biological approach to bone regeneration would be the development of a synthetic material with intrinsic osteoinductive capacity. Earlier on, Winter and Simpson reported bone formation upon implantation of a polyhydroxyethylmethacrylate sponge under the skin of pigs, an experiment performed in an attempt to explain incidences of hard tissue formation upon implantation of synthetic breast implants (16). In the past 30 years, several porous calcium phosphate biomaterials as well as some metals were reported to possess osteoinductive capacity (17). The underlying mechanism leading to bone induction by synthetic materials remains largely unknown; however, osteoinductive potential of biomaterials can be controlled by tailoring material characteristics such as chemical composition, surface topography, and geometry, which in turn affect resorption rate and cell-material interactions.

The aim of this study was to correlate the osteogenic potential of a family of porous ceramic materials in vitro to ectopic bone formation in vivo and to demonstrate that synthetic materials present a bona fide alternative to autograft and BMP therapy with equal performance in the healing of a critical-size bone defect.

Results

Synthesis and Characterization of Calcium Phosphate Ceramics. In order to produce porous calcium phosphate ceramics with varying biological activities, we either used calcium phosphate powder with different chemical compositions (hydroxyapatite [HA], tricalcium phosphate [TCP], or a mixture thereof [biphasic calcium phosphate, BCP]) or we exposed the ceramics to different post-synthesis sintering temperatures (BCP1150 sintered at 1150 °C and BCP1300 sintered at 1300 °C) to obtain materials with equal chemistry but varying microstructure. Using X-ray diffraction (XRD) analysis, we observed the presence of β-TCP in BCP and a trace of HA (<10 wt %) in TCP, whereas HA was phase-pure (Fig. 1*A*). Image analysis on cross-section showed no differences in macrostructure among different ceramics, though the micropore size and volume varied (Fig. S1 *A* and *B*). The average grain size of BCP1150 and TCP was smaller and the number of micropores higher as compared to HA and BCP1300 as shown by SEM (Fig. 1*B*). As a consequence, the specific surface area of the four ceramics varied from 0.1 m^2/g for HA to 1.2 m^2/g for TCP, resulting in differences in adsorption of serum proteins,

Author contributions: H.Y., H.F., P.H., J.d.B., C.A.v.B., and J.D.d.B. designed research; H.Y., H.F., A.M.C.B., A.d.R., and W.R.W. performed research; H.Y. contributed new reagents/analytic tools; H.Y., H.F., J.d.B., A.M.C.B., A.d.R., W.R.W., and J.D.d.B. analyzed data; and H.F., P.H., and J.d.B. wrote the paper.

Conflict of interest statement: H.Y., J.D.d.B., and C.A.v.B. are share-holders of Progentix Orthobiology.

*This Direct Submission article had a prearranged editor.

[1]H.Y. and H.F. contributed equally to this work.

[2]To whom correspondence should be addressed. E-mail: j.d.debruijn@qmul.ac.uk.

This article contains supporting information online at www.pnas.org/lookup/suppl/doi:10.1073/pnas.1003600107/-/DCSupplemental.

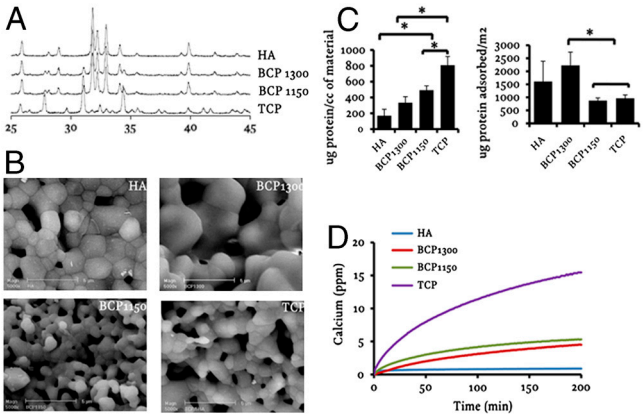

Fig. 1. Characterization of calcium phosphate ceramics. (*A*) XRD analysis showing the composition of the four different ceramics with their characteristic peaks indicated. (*B*) Environmental SEM photographs depicting their microstructure. (*C* and *D*) Protein adsorption and calcium release profile of the different ceramics, respectively. The error bars represent standard deviations. An asterisk (*) denotes statistical difference (one-way Anova and Tukey's test, $P < 0.05$).

with TCP adsorbing more proteins per volume of material than BCP1150 and BCP1300 (Fig. 1*C*). In contrast, when adsorption of protein was expressed per surface area, BCP1150 and TCP bound less proteins than BCP1300 and HA. Despite variations in the quantity, no qualitative differences were observed in the type of proteins adsorbed on different ceramics (Fig. S1*C*). We assessed the rate of calcium release from the four ceramics and found that it was significantly faster for TCP compared to the other three ceramics (Fig. 1*D*). An overview of the materials characteristics is given in Table 1.

Materials Support Osteogenic Differentiation of Human Bone Marrow-Derived Multipotent MSCs. The effect of material properties on tissue development is mediated via cell-material interaction and therefore we decided to analyze the effect of the four different materials on osteogenic differentiation of human multipotent marrow stromal cells (hMSCs) in vitro and in vivo (18, 19). First, we seeded hMSCs [previously tested for their multipotency and phenotypically characterized following protocols described elsewhere (20); see Figs. S2 and S3] on the four different ceramics and cultured them for 7 d in osteogenic differentiation medium, after which quantitative PCR was performed on a panel of genes indicative of osteogenic differentiation. As a control, we grew hMSCs on tissue culture flasks in control and osteogenic medium and observed the well-documented increase in alkaline phosphatase (ALP) expression in osteogenic medium (Fig. S4) (21). With the exception of ALP and collagen type I, gene expression of all genes was higher on the four ceramics than on tissue culture flasks, suggesting that the ceramics favor osteogenic differentiation (Fig. 2*A* and Fig. S4) Furthermore, marked differences in expression levels of genes encoding osteocalcin, bone sialoprotein, and osteopontin were found in hMSCs cultured on the different ceramics. A similar but less profound effect for S100A4 and Runx2 was also observed. Interestingly, hMSCs on TCP consistently displayed the most osteogenic profile, and on HA the least (Fig. S4).

Next, we assessed bone apposition by hMSCs on the different ceramics. Porous calcium phosphate ceramics are frequently used in bone tissue-engineered constructs, in which culture expanded MSCs are seeded onto the ceramic in vitro and then implanted. Upon implantation, MSCs will differentiate into osteoblasts and deposit bone tissue onto the ceramic surface (22). We cultured hMSCs in vitro for 7 d on the four calcium phosphate ceramics (HA, BCP1300, BCP1150, and TCP) in osteogenic medium. The constructs were implanted subcutaneously into immunodeficient mice for 6 weeks after which formation of new bone tissue was assayed using histomorphometry. No bone formation was observed either on scaffolds without cells or on HA scaffolds seeded with hMSCs (Fig. 2 *B* and *C*). In contrast, we did observe apposition of bone tissue on grafts of BCP1300, BCP1150, and TCP ceramics seeded with hMSCs. On TCP, we observed a 5 times higher amount of bone than on BCP1300 and BCP1150 ($2.7 \pm 1.6\%$ in TCP, $0.7 \pm 1.3\%$ in BCP1300, and $0.6 \pm 0.9\%$ in BCP1150), demonstrating that ceramics stimulated osteogenic differentiation in vitro and bone formation in vivo depending on their physicochemical and structural characteristics.

In Vivo Osteoinduction by Different Calcium Phosphate Ceramics. As mentioned before, osteoinduction is a critical parameter of any bone graft in large bone defects. To analyze the osteoinductive potential of our ceramics, we used both ectopic implantation in muscle tissue of eight dogs and the clinically relevant posterolateral spinal fusion model in which two materials can be compared in a paired manner. For this purpose, we selected the two extremes from the previous experiments, HA and TCP. Histomorphometric analysis after 12 weeks of implantation showed that the area percentage of bone in available pore space was 5 times higher in TCP as compared to HA, both in muscle and in the spine, demonstrating that calcium phosphate ceramics with different chemical composition have different osteoinductive potential, which was in accordance with in vitro results (Fig. 3 *A* and *B*). We observed a resorption of 77% of the im-

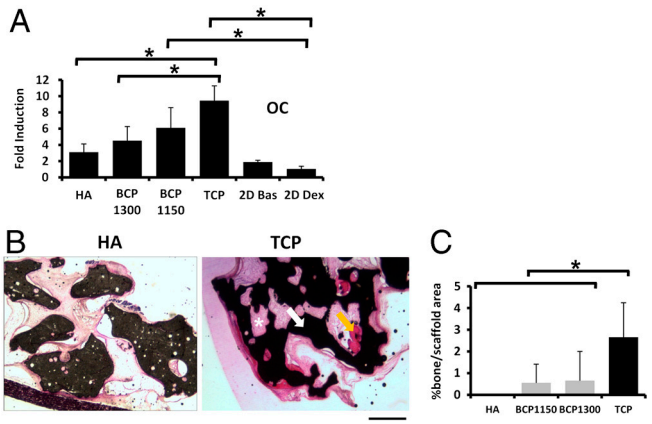

Fig. 2. Osteogenic differentiation of hMSCs on ceramics of different composition. (*A*) Expression of the bone-related protein osteocalcin by hMSCs seeded in the different ceramics. Expression levels were normalized with 18S. Fold induction was calculated using the ΔCT method relative to dex-treated hMSCs in tissue culture plates. The error bars represent standard deviations. *B* and *C* indicate the bone forming potential of hMSCs seeded in different ceramics. Histological sections (*B*) and quantification of bone area per scaffold area (*C*) are shown. Basic Fuchsin stains bone red (orange arrow), methylene blue stains fibrous tissue blue (*), and the ceramic is shown in black (white arrow). The error bars represent standard deviations. An asterisk (*) denotes statistical difference (one-way Anova and Tukey's test, $P < 0.05$). (Scale bar: 200 μm.)

Table 1.

	HA	TCP	BCP1150	BCP1300
Chemistry	HA	5HA + 95TCP	20TCP/80HA	20TCP/80HA
Particle size, mm	1–2	1–2	1–2	1–2
Specific surface, m^2/g	0.1	1.2	1	0.2
Percentage of materials, %	46.4 ± 2.4	49.9 ± 1.8	45.6 ± 2.2	44.6 ± 1.9
Microporosity, %*	3.1	48.7	41.1	8.7
Ca release, ppm	0.9 ± 0.1	15.3 ± 0.2	5.4 ± 0.1	4.2 ± 0.4

*Volume percentage of micropores smaller than 10 μm within the ceramic.

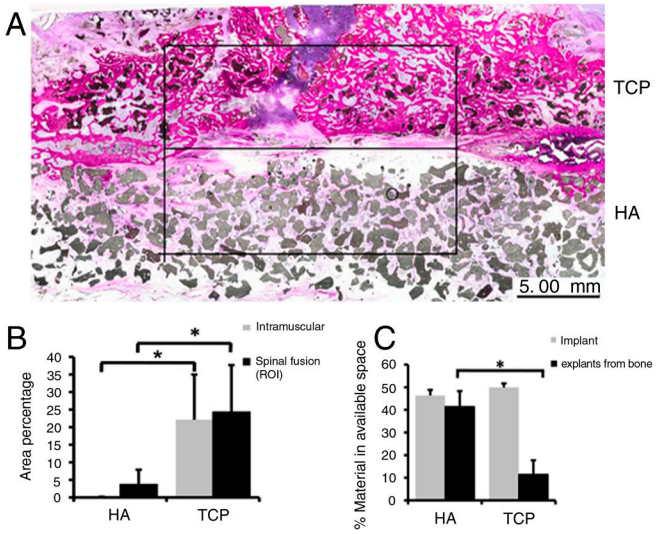

Fig. 3. Posterolateral spinal fusion in dogs. (*A*) Histological overviews showing newly formed bone in TCP and HA implants (square, region of interest). (*B*) The area percentage of bone for HA and TCP ceramics in the case of intramuscular implantation (gray bars) and in the spinal fusion (black bars). (*C*) The percentage of material available before implantation (gray bars) and upon explantation (black bars). Note that HA ceramic was not resorbed during the 12 weeks implantation in contrast with TCP. The error bars represent standard deviations. An asterisk (*) denotes statistical difference (Student's paired *t* test, $P < 0.05$).

planted TCP after 12 weeks of implantation, whereas no detectable resorption of HA was found (Fig. 3*C*).

To demonstrate that not only chemistry but also structural characteristics can influence the osteoinductive potency of ceramics, we implanted BCP1150, BCP1300, and TCP in muscle of ten sheep. Unfortunately, HA was omitted from this study due to technical difficulties. Twelve weeks after implantation in paraspinal muscles, we observed that bone induction had occurred in all three calcium phosphate ceramics; however, the amount of bone formed varied among the different ceramics (Fig. 4*A*). Bone apposition was again highest in TCP ($28.7 \pm 4.8\%$ of available pore space) followed by BCP1150 ($17.7 \pm 5\%$). Significantly less bone was observed in BCP1300 ($11 \pm 7.5\%$) indicating that both chemistry and structural properties can influence the in vivo osteoinductive potential of the ceramics (Fig. 4*B*).

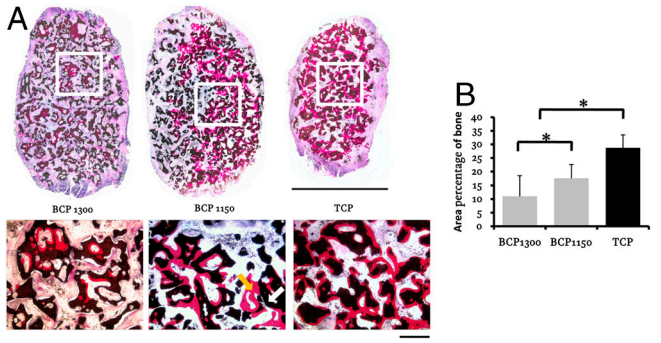

Fig. 4. Osteoinductive potential of different calcium phosphate ceramics implanted intramuscularly in sheep. (*A*) Histological sections showing the newly formed bone (orange arrow) and the calcium phosphate ceramic (white arrow) upon 12 weeks implantation. Basic Fuchsin stains the newly formed bone red, methylene blue stains fibrous tissue blue, and the scaffold is shown in black. (*B*) Quantification of newly formed bone. The error bars represent standard deviations. An asterisk (*) denotes statistical difference (one-way Anova and Tukey's test, $P < 0.05$). (*Top*, Scale bar: 10 mm.) (*Bottom*, Scale bar: 200 μm.)

Calcium Phosphate Ceramics as a Bone Graft Substitute in a Critical-Size Defect. The studies above indicate that TCP is a superior ceramic with respect to stem cell differentiation and osteoinduction in vivo. We next tested the ability of TCP to heal a critical-sized orthotopic defect in comparison with standard treatments. To this end, we implanted TCP in a bilateral iliac wing defect in sheep with a critical-size diameter of 17 mm. As a negative control, we included a group in which the defect was left empty, and as a positive control, we used two groups of sheep in which the defect was either treated with autologous bone or with a preparation of recombinant human BMP-2 (rhBMP-2) delivered in a collagen sponge (Infuse® Bone Graft, Medtronic). The latter treatment is a commercially available product used for spinal fusion surgery (23, 24).

Twelve weeks after implantation, we observed that the iliac wing defect was not able to heal spontaneously, although some newly formed bone could be seen along the host bone bed ($3.1 \pm 1.8\%$ of the defect was covered with bone; Fig. 5 and Fig. 6), confirming that the defect was critically sized (25). In contrast, when autologous bone was used as an implant, bone was found throughout the defect ($32.2 \pm 6.5\%$). As it is difficult to distinguish between implanted bone autograft and newly formed bone, the percentage of bone measured represents both residual bone autograft and newly formed bone. Histological analysis revealed tight bonding between new bone and the host bone bed, without interspersed fibrous tissue layer (Fig. 6). However, in the center of the defect, less bone was observed than in the defect periphery, and large areas were filled with fibrous tissue in all animals tested. Results obtained upon implantation of rhBMP-2 were similar to those of autologous bone. In the rhBMP-2 treated defects, $22.8 \pm 10.1\%$ of the defect was filled with new bone. Fibrous tissue was observed in the center of the defect of all animals tested. In addition, ectopic bone formation outside the defect area was found in 8 out of 10 animals, probably due to diffusion of rhBMP-2 from the graft into the adjacent soft tissue (Fig. 5).

Interestingly, implants made of TCP ceramic showed similar performance to autologous bone regarding bone formation. With an area of new bone covering $33.9 \pm 6.8\%$ of the defects, they outperformed the rhBMP-2 group, an overview of the histology and quantification of bone formation can be seen in Fig. 6 *A* and *B*,

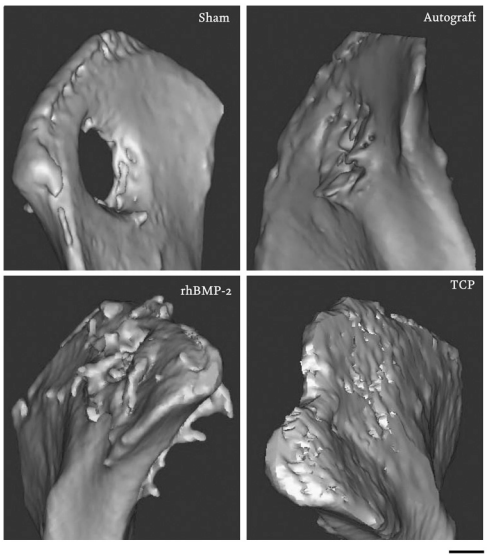

Fig. 5. Illium defect. Figure presents three-dimensional models of the os ilium after 12 weeks implantation. Bone formation outside the margins of the defect was found in the rhBMP-2 group, whereas in the TCP group, the material remained within the defect with new bone formation and implant resorption observed at 12 weeks.

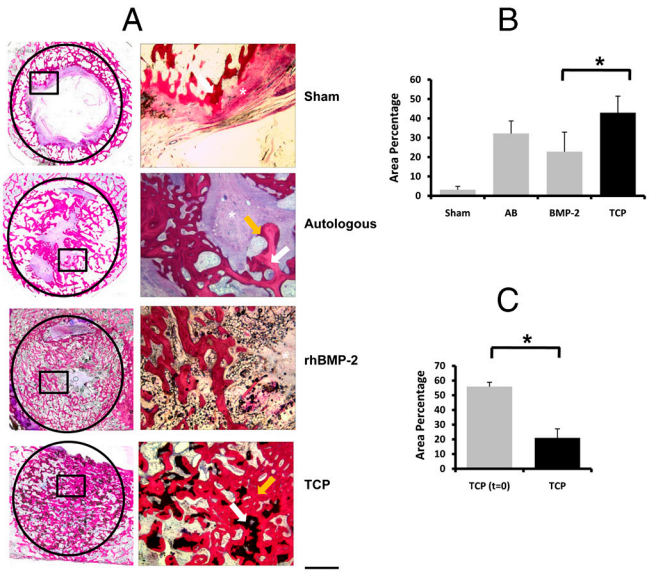

Fig. 6. Performance of calcium phosphate ceramics, autologous bone, and rhBMP-2 in a critical-size defect in the illium of sheep. (*A*) Histological sections depicting the newly formed bone within the defect created in the illium of sheep. The defect margins are indicated by the black circle (17 mm in diameter) on the left panel and on the right panel the demarked region can be seen in detail. Basic fuchsin stains bone red, methylene blue stains fibrous tissue blue, and the scaffold is shown in black. Newly formed bone is indicated by an orange arrow, autologous bone or the ceramic material are indicated by a white arrow, and fibrous tissue is indicated by an asterisk (*). *B* and *C* represent the area percentage of bone per available area between the different conditions (*B*) and the resorption of the ceramic after 12 weeks implantation (*C*). The error bars represent standard deviations. An asterisk (*) denotes statistical difference (one-way Anova and Tukey's test, $P < 0.05$ (*B*) and Student's paired *t* test, $p < 0.05$ (*c*). (Scale bar: 200 μm.)

respectively. Significant resorption of the ceramic material could be observed: The percentage of ceramic area in the defect area decreased from 56% to 21% after 12 weeks of implantation (Fig. 6*C*). Similar to autograft, new bone formed in TCP treated defect formed a tight bond with the host bone, and no fibrous tissue was observed in the periphery of the defect. In the central area of the defect, only 2 out of 10 animals showed the presence of fibrous connective tissue.

Discussion

The fully synthetic implant based on calcium phosphate ceramic reported in this study was at least equally successful to autograft and rhBMP-2 in the treatment of a critical-sized bone defect. Unlike many other synthetic bone graft substitutes, which are considered solely osteoconductive, the ceramic presented here possesses intrinsic osteoinductivity, comparable to autograft, DBM, and BMPs. This intrinsic osteoinductivity could, in part, explain its performance orthotopically and represent a paradigm shift in the treatment of bone defects.

So far, porous ceramics are used as bone fillers for small bone defects, where osteoconduction is sufficient. Autograft is still the prime choice in treatment of complex and large bone defects considering the autologous nature as well as strong clinical performance. Although BMPs are potent molecules and represent an alternative to autograft, limitations remain in terms of dose, release kinetics, and mechanical properties, as mentioned earlier. Annually, around 300,000 patients undergo spinal fusion procedures in United States alone with estimated costs of $11.25 billion involving mainly autologous bone grafting and BMPs. In our study, TCP proved equally efficient as autologous bone in inducing bone apposition in the preclinical iliac wing defect model in sheep, with even less fibrous tissue in the central regions of the implant than autologous bone. Fibrous tissue formation is one of the main reasons for unsuccessful healing of large bone defects and nonunions as well as for implant failure. Bone formation induced by TCP remained within regions of the defect, whereas we observed BMP-induced bone formation in soft tissue surrounding the defect as well. Based on the findings reported in this paper, we have embarked on clinical trials to evaluate the possibility of using TCP as a true bone graft in large bone defects.

Our data show that the ability of ceramics to instruct cell and tissue development can be controlled merely by changing either the chemical composition or structural properties. The calcium phosphate ceramic formulations investigated in this study represent a process of optimization in the search for an optimal alternative to autograft. First, chemistry was varied from pure HA, to a mixture of HA and TCP (BCP), and finally to TCP with traces of HA. Second, the macrostructure of the four ceramics was kept equal for the four ceramics. Presence of macrostructural features, such as macropores (26–28), concavities/channels (29, 30), or voids between particles (31) has previously been shown to be a prerequisite for osteoinduction by synthetic biomaterials. By keeping the macroporosity of the four ceramics similar, we attempted to avoid the effect of this parameter on the osteoinductive potential of the ceramics. Finally, microstructural properties were controlled by the processing parameters: Microstructural surface properties of the two BCPs, with equal chemistry and macrostructure, were varied by controlling their sintering temperature. Significant differences in osteoinductive potential were observed between the BCPs sintered at 1150 and 1300 °C: An increase in microporosity and a decrease in grain size, resulting in an increase of the specific surface area of the ceramic, was shown to render a ceramic osteoinductive (32). Similarly, a comparison between HA and BCP, sintered at the same temperature, thus with similar macro- and microstructural features but different chemistry, showed a more pronounced bone formation in BCP, which contains highly resorbable TCP (33). The suggestion that both an increase in specific surface area and an increase in resorbability of a ceramic may be beneficial for its osteoinductive potential eventually led to the development of a calcium phosphate ceramic with higher TCP content and higher surface area—the TCP formulation presented herein. Many other formulations can be developed; however, the processing parameters and the fact that osteoinduction is mainly observed in large animals limit the number of formulations to be tested. The high osteoinductive potential of TCP begs questions about the cellular and molecular mechanism behind it. Although we have not pinpointed a particular signal transduction pathway yet, the fact that TCP shows higher expression of osteogenic markers by hMSCs in vitro and more de novo bone formation in vivo as compared to other investigated ceramics suggests a mechanism in which TCP triggers osteogenic differentiation. Our working hypothesis is that pericytes, the smooth muscle cells aligning the invading capillary blood vessels, encounter a milieu in which the cells differentiate into osteoblasts (34). We are testing the hypothesis by focussing on the interaction between TCP and hMSCs in vitro and in the ectopic bone formation model using microarray analysis and genetic interference studies. Another remaining question concerns the other side of the molecular interface: Which biomaterial properties play a role in osteoinductivity and how do they influence the osteogenic process? Differences in dissolution behavior of the ceramic, which can be obtained either by changes in chemical composition (calcium phosphate phase) or by changes in structural properties (crystallinity, grain size, porosity, specific surface area) seem to be associated with osteoinductive potential in vivo (17). We observed that the ceramic with the strongest osteoinductive potential displays the most pronounced dissolution in vitro and degradation in vivo. It is plausible to think that the calcium release plays a role in the process but further studies are needed to identify the responsive cell types and the pathways activated by calcium. Similarly, we observed differences in in vitro protein adsorption with TCP as

the ceramic with the highest protein adsorption per volume of all ceramics. Nevertheless, despite these quantitative differences, we did not observe differences regarding the nature of the proteins adsorbed by the four ceramics. It is important to investigate whether the higher protein content of TCP reflects changes in the ratio pro/antiosteogenic proteins and, if so, which proteins are involved in the process. However, it should be emphasized that differences in protein adsorption do not necessarily have a causal relationship with osteoinductive potential in vitro and in vivo.

Resolving the molecular mechanism of osteoinduction will offer tools to develop new osteoinductive materials, e.g., based on polymeric materials, in order to meet other requirements for successful bone repair, such as mechanical and handling properties. Furthermore, by understanding biological processes involved in osteoinduction by biomaterials, we will obtain more fundamental insight into biomaterial–tissue interactions.

Data presented in this manuscript on ceramic biomaterials in the area of bone graft substitution provide preclinical proof of concept for a generation of smart materials, displaying superior biological performance through modulation of cell behavior. Bioinstructive materials can find their way in a plethora of applications, from biodegradable sutures to contact lenses and stents, and in all instances, the challenge lies in finding the optimal parameters for the particular biomedical application. To do so, in vitro bioassays that predict the performance of a material for intended application in the human body are essential. In this manuscript, the prospective knowledge of the osteoinductive capacity of different ceramics helped us in identifying a suitable in vitro cell system. For other biomaterials and other clinical applications, cell biologists and material scientists need to team up to streamline the process of identifying tissue instructive biomaterial properties.

Materials and Methods

Synthesis and Characterization of Calcium Phosphate Ceramics. HA ceramics were prepared from HA powder (Merck) using the dual-phase mixing method and sintered at 1250 °C for 8 h according to a previously described method (35). BCP ceramics were fabricated using the H_2O_2 method using in-house-made calcium-deficient apatite powder and sintered at 1150 °C (BCP1150) and 1300 °C (BCP1300), respectively (36). The method used to synthesize the BCP ceramics was also used for preparation of TCP. TCP ceramics were prepared from TCP powder (Plasma Biotal) and sintered at 1100 °C. Ceramic particles (1–2 or 2–3 mm) were prepared, cleaned ultrasonically with acetone, 70% ethanol and demineralized water, dried at 80 °C, and sterilized by gamma irradiation prior to use.

The macro- and microstructure of the different ceramics was evaluated using an SEM (XL30, Environmental SEM-Field Emission Gun, Philips). Composition of the ceramics was determined by XRD (Miniflex). Specific surface area of the different ceramics was analyzed with mercury intrusion (Micromeritics Instrument, Inc.).

The calcium release profile of the ceramics was determined by immersing 0.5 mL of 1–2 mm ceramic particles in 100 mL of simulated physiological saline (0.8% NaCl, 50 mM Hepes, 37 °C, pH 7.3) and monitoring the calcium concentration using a calcium electrode for 200 min.

To calculate the concentration of protein adsorbed, 1 mL of ceramic particles was incubated for 3 d in 1% FBS in PBS at 37 °C. Protein adsorption was measured using a protein assay kit (micro-bicinchoninic acid™, Perbio) according to the manufacturer's protocol. Analysis of the proteins adsorbed to the different ceramics was performed using gel separation by electrophoresis after incubation of the ceramics for 1 d in serum. Equal amounts of proteins were loaded onto the gel and, upon separation, the gel was stained with Coomassie blue.

RNA Isolation and Quantitative PCR. To analyze the effect of the different ceramics in the gene expression profile of hMSCs, 2×10^5 cells were seeded per three particles and cultured for 7 d in osteogenic medium. As a control, we seeded 5,000 cells/cm^2 on tissue culture flasks either in basic or osteogenic medium for 7 d. Total RNA was isolated using Trizol and the Nucleospin RNA isolation kit (Macherey-Nagel) according to the manufacturer's protocol. The quality and quantity of RNA was analyzed by gel electrophoresis and spectrophotometry. Six hundred and fifty nanograms of RNA was used for cDNA synthesis using iScript cDNA synthesis kit (BioRad) according to the manufacturer's protocol. PCR was performed on a Light Cycler real-time PCR machine (Roche) using SYBR® green I master mix (Invitrogen). Data was analyzed using Light Cycler software version 3.5.3, using fit point method by setting the noise band to the exponential phase of the reaction to exclude background fluorescence. Fold induction relative to cells grown on tissue culture flasks in osteogenic medium was calculated using the ΔCT method after normalization with 18S as a housekeeping gene.

Ectopic Bone Formation by hMSCs. hMSCs were isolated from adult bone marrow and cultured as previously described (37). To evaluate the effect of different calcium phosphate ceramics on ectopic bone formation by hMSCs, we seeded 2×10^5 cells per three particles of approximately 2–3 mm. Cells were cultured in vitro for 7 d in the presence of osteogenic medium. Prior to implantation, the tissue-engineered constructs were washed with PBS. Six immunodeficient mice (HsdCpb:NRI-nu, Harlan) were anesthetized using isoflurane, surgical sites were cleaned with ethanol, and four subcutaneous pockets created. Three particles of each of the calcium phosphate ceramics were implanted in these pockets for 6 weeks.

Posterolateral Spinal Fusion Model in Dog. The experiments were performed following approval of local Animal Care and Ethics Committee (Animal Center, Sichuan University, Chengdu, China). The surgical operation was performed under general anaesthesia (30 mg pentobartital sodium per kilogram body weight) and sterile conditions. Firstly, the spinous processes of L3 an L4 were identified, and small bilateral incisions were made. Secondly, the spinous processes and the vertebral body between L3 and L4 were exposed in both sides by blunt separation. After injuring the exposed bone using a scraper, materials (HA or TCP, 1–2 mm, 5 mL) were placed in both sides. Finally, the muscles from both sides were tightly closed with sutures. After surgery, penicillin was intramuscularly injected for three consecutive days to prevent infection. In addition, 1 mL of ceramic particles of HA and TCP were implanted in paraspine muscle to evaluate the osteoinductive potential of the ceramics in this model. Twelve weeks after surgery, the animals were killed and samples were harvested with surrounding tissues. The samples were then fixed, dehydrated, embedded in methyl methacrylate (MMA), and undecalcified sections were made parallel to the posterolateral processes and stained with methylene blue and basic fuchsin for histological and histomorphometrical analysis. Sections obtained 5 mm away from the end of spinous processes were used for histomorphometry and the area between the two processes and 5 mm from the middle was selected as region of interest. The area percentage of bone in the region of interest and in available space, and area percentage of materials in region of interest, were calculated and data obtained from eight animals were pooled for quantitative analyses.

Sheep Model (Intramuscular Implantation and Iliac Implantation). All the experiments were performed following approval of the University Animal Care and Ethics Committee from the University of New South Wales, Randwick, Australia.

Ten adult female sheep (3 years old) were used for intramuscular (ectopic) implantation. Different calcium phosphate ceramic (BCP1300, BCP1150, and TCP) particles with a size of 1–2 mm were implanted intramuscularly in separate pockets for 12 weeks. For the iliac implantation (orthotopic implantation), 22 adult female sheep (3 years old) were sedated using an intramuscular injection of Zoletil and anesthetized using a mixture of O_2 (4 L/min) and isoflurane (1.5–2.5%). Pain relief was administered prior to commencement of the surgical procedure. An incision was made over the exposed length of both iliac crests, through the periosteum. Upon exposure of the os ilium, a 17-mm defect was created and the implants (autograft, rhBMP-2, or TCP) were placed into the defects. The periosteum, muscles, fat tissue, and skin were closed over the iliac crest by suturing layers using resorbable sutures (3-0 Dexon, Davis and Geck). In the case of autograft, the bone was harvested at the same time as the creation of the defect and reduced to 1–2-mm particles using a rongeur. Recombinant human BMP-2 (Medtronic) at a concentration of 0.4 mg/mL (0.72 mg/defect) was soaked on 17-mm-diameter Helistat absorbable collagen hemostatic sponges (Integra LifeSciences Corp.) for 15 min prior to stacking in the defect.

During the implantation period, animals were fed with a standard diet and had continuous access to water.

Histology and Histomorphometry. Implants were retrieved and fixed in 0.14 M cacodylic acid buffer pH 7.3 containing 1.5% glutaraldehyde. Fixed samples were dehydrated in ethanol series and embedded in MMA. Sections were processed on a histological diamond saw (Leica SP1600) and stained with 1% methylene blue (Sigma) and 0.3% basic fuchsin solution (Sigma).

Sections (one section per sample across the middle, or otherwise specified) were scanned using a digital scanner (Dimage Scan Elite 5400II, Konica Minolta Photo Imaging, Inc.) to obtain an overview, and representative images were used for histomorphometrical analysis using Photoshop software (Adobe). Either the area percentage of bone in the samples or the area percentages of bone in the available space were obtained for quantitative analyses.

Statistical Analysis. Statistical analysis was performed using a one-way ANOVA followed by a Tukey's multiple comparison test or paired *t* test ($P < 0.05$). All animals mentioned in the experimental setup were used for statistical analysis. No incidents were registered during the course of animal experiments.

ACKNOWLEDGMENTS. We would like to thank Linda van Rijn and Ruiqing Wang for technical support. The authors acknowledge the support of the Smart Mix Program of The Netherlands Ministry of Economic Affairs and The Netherlands Ministry of Education, Culture and Science (A.M.C.B. and J.d.B.), Senter Novem (H.F., H.Y.), and the Innovative Research Incentives Scheme Veni of The Netherlands Organisation for Scientific Research (P.H.).

1. Chen CS, Mrksich M, Huang S, Whitesides GM, Ingber DE (1997) Geometric control of cell life and death. *Science* 276(5317):1425–1428.
2. Engler AJ, Sen S, Sweeney HL, Discher DE (2006) Matrix elasticity directs stem cell lineage specification.. *Cell* 126(4):677–689.
3. McBeath R, Pirone DM, Nelson CM, Bhadriraju K, Chen CS (2004) Cell shape, cytoskeletal tension, and RhoA regulate stem cell lineage commitment. *Dev Cell* 6(4):483–495.
4. Folkman J, Moscona A (1978) Role of cell shape in growth control. *Nature* 273(5661):345–349.
5. Place ES, Evans ND, Stevens MM (2009) Complexity in biomaterials for tissue engineering. *Nat Mater* 8(6):457–470.
6. Dalby MJ, et al. (2007) The control of human mesenchymal cell differentiation using nanoscale symmetry and disorder. *Nat Mater* 6:997–1003.
7. Moroni L, Licht R, de Boer J, de Wijn JR, van Blitterswijk CA (2006) Fiber diameter and texture of electrospun PEOT/PBT scaffolds influence human mesenchymal stem cell proliferation and morphology, and the release of incorporated compounds. *Biomaterials* 27(28):4911–4922.
8. Kohn J (2004) New approaches to biomaterials design. *Nat Mater* 3(11):745–747.
9. Urist MR (1965) Bone: Formation by autoinduction. *Science* 150(3698):893–899.
10. Friedenstein AY (1968) Induction of bone tissue by transitional epithelium. *Clin Orthop Relat Res* 59:21–37.
11. Damien CJ, Parsons JR (1991) Bone graft and bone graft substitutes: A review of current technology and applications. *J Appl Biomater* 2(3):187–208.
12. Wang J, et al. (2007) A comparison of commercially available demineralized bone matrix for spinal fusion. *Eur Spine J* 16(8):1233–1240.
13. Drosos GI, Kazakos KI, Kouzoumpasis P, Verettas D-A (2007) Safety and efficacy of commercially available demineralised bone matrix preparations: A critical review of clinical studies. *Injury* 38(Suppl 4):S13–S21.
14. Bormann N, Pruss A, Schmidmaier G, Wildemann B (2010) In vitro testing of the osteoinductive potential of different bony allograft preparations. *Arch Orthop Traum Surg* 130:143–149.
15. Garrison KR, et al. (2007) Clinical effectiveness and cost-effectiveness of bone morphogenetic proteins in the non-healing of fractures and spinal fusion: A systematic review. *Health Technol Asses* 11(30):1–150.
16. Winter GD, Simpson BJ (1969) Heterotopic bone formed in a synthetic sponge in the skin of young pigs. *Nature* 223(5201):88–90.
17. LeGeros RZ (2008) Calcium phosphate-based osteoinductive materials. *Chem Rev* 108(11):4742–4753.
18. Pittenger MF, et al. (1999) Multilineage potential of adult human mesenchymal stem cells. *Science* 284(5411):143–147.
19. Bianco P, Robey PG (2001) Stem cells in tissue engineering. *Nature* 414(6859):118–121.
20. Fernandes H, et al. (2009) Endogenous collagen influences differentiation of human multipotent mesenchymal stromal cells. *Tissue Eng Pt A* 16(5):1693–1702.
21. Siddappa R, et al. (2008) cAMP/PKA pathway activation in human mesenchymal stem cells in vitro results in robust bone formation in vivo. *Proc Natl Acad Sci USA* 105(20):7281–7286.
22. Crane GM, Ishaug SL, Mikos AG (1995) Bone tissue engineering. *Nat Med* 1(12): 1322–1324.
23. Boden SD, Zdeblick TA, Sandhu HS, Heim SE (2000) The use of rhBMP-2 in interbody fusion cages. Definitive evidence of osteoinduction in humans: A preliminary report. *Spine* 25(3):376–381.
24. Burkus JK, Gornet MF, Dickman CA, Zdeblick TA (2002) Anterior lumbar interbody fusion using rhBMP-2 with tapered interbody cages. *J Spinal Disord Tech* 15(5): 337–349.
25. Anderson ML, et al. (1999) Critical size defect in the goat's os ilium. A model to evaluate bone grafts and substitutes. *Clin Orthop Relat Res* 364:231–239.
26. Gosain AK, et al. (2002) A 1-year study of osteoinduction in hydroxyapatite-derived biomaterials in an adult sheep model: Part I. *Plast Reconstr Surg* 109(2):619–630.
27. Yamasaki H, Sakai H (1992) Osteogenic response to porous hydroxyapatite ceramics under the skin of dogs. *Biomaterials* 13(5):308–312.
28. Klein C, de Groot K, Chen W, Li Y, Zhang X (1994) Osseous substance formation induced in porous calcium phosphate ceramics in soft tissues. *Biomaterials* 15(1): 31–34.
29. Ripamonti U, Crooks J, Kirkbride AN (1999) Sintered porous hydroxyapatites with intrinsic osteoinductive activity: Geometric induction of bone formation. *S Afr J Sci* 95(8):335–343.
30. Habibovic P, et al. (2008) Osteoconduction and osteoinduction of low-temperature 3D printed bioceramic implants. *Biomaterials* 29(7):944–953.
31. Le Nihouannen D, et al. (2006) Micro-architecture of calcium phosphate granules and fibrin glue composites for bone tissue engineering. *Biomaterials* 27(13):2716–2722.
32. Habibovic P, Sees TM, van den Doel MA, van Blitterswijk CA, de Groot K (2006) Osteoinduction by biomaterials—physicochemical and structural influences. *J Biomed Mater Res A* 77(4):747–762 (in eng).
33. Habibovic P, et al. (2005) 3D microenvironment as essential element for osteoinduction by biomaterials. *Biomaterials* 26(17):3565–3575.
34. da Silva Meirelles L, Caplan AI, Nardi NB (2008) In search of the in vivo identity of mesenchymal stem cells. *Stem Cells* 26(9):2287–2299.
35. Li S, De Wijn JR, Li J, Layrolle P, De Groot K (2003) Macroporous biphasic calcium phosphate scaffold with high permeability/porosity ratio. *Tissue Eng* 9(3):535–548.
36. Yuan H, et al. (2002) A comparison of the osteoinductive potential of two calcium phosphate ceramics implanted intramuscularly in goats. *J Mater Sci: Mater Med* 13(12):1271–1275.
37. de Bruijn JD, et al. (1999) Bone induction by implants coated with cultured osteogenic bone marrow cells. *Adv Dent Res* 13:74–81.